Characterization of the Propagation Route of Light Passing Through Convex Lens

Jiafa Mao (maojiafa@zjut.edu.cn)
Zhejiang University of Technology
Weiguo Sheng (w.sheng@ieee.org)
Hangzhou Normal University
Yahong Hu
Zhejiang University of Technology
Kejie Mao
Zhejiang University of Technology
Hua Gao
Zhejiang University of Technology
Ronghua Liang
Zhejiang University of Technology

Research Article

Keywords: Light passing through the convex lens (LPCL), Angular affine transformation (AAT), Pinhole imaging, Normal direction, Ratio of focal length to radius (RFR)

Posted Date: January 5th, 2022

DOI: https://doi.org/10.21203/rs.3.rs-1213027/v1

Characterization of the Propagation Route of Light Passing Through Convex Lens

Jiafa Mao[1]✉, Weiguo Sheng[2]✉, Yahong Hu[1], Kejie Mao[1], Hua Gao[1], Ronghua Liang[1]

Abstract: Existing optical theory states that the light directed to the optical center of the convex lens will travel in a straight line. Does the theory hold? If this is true, then why the images formed by the camera lens tends to be distorted? To answer the question, this paper studied the propagation mode of light passing through convex lens. Specifically, assuming the propagation medium on both sides of convex lens is homogeneous, we propose an angular affine transformation (AAT) theory. Based on the proposed theory, we first derive the refractive index of convex lens as well as the method of calculating the normal direction of each point within the radius of convex lens radius and then derive the refraction direction of each point within the radius of convex lens, thus completely characterizing the path diagram of light directed to the optical center. The correctness of the proposed theory has been verified using two sets of experiments: characterization of the route of light passing through the convex lens as well as camera imaging experiment. From the results, it can be concluded that the light directed to the optical center of convex lens does not travel in a straight line, but in a refraction line.

Keywords: Light passing through the convex lens (LPCL), Angular affine transformation (AAT), Pinhole imaging, Normal direction, Ratio of focal length to radius (RFR).

1. Introduction

The development of optical engineering characterizes the progress of human civilization. Optics, as the backbone of physics, has been well studied, leading to geometric optics [1], wave optics [2], quantum optics [3] and nonlinear optics [4]. It reveals the law of light generation and propagation and its interaction with matter. Optical engineering involves in optical instrument design, such as lenses, microscopes and telescopes [5]. In addition, optical engineering also studies optical sensors and related measurement systems, lasers, optical fiber communications, and optical discs [6,7]. Recently, the employment of imaging principles to study precision measurement [8] and visual navigation [9,10], has become an important research direction, which is also critical for artificial intelligence research.

In machine vision, acquisition of 3D depth information is a challenging issue in the areas of autonomous navigation of intelligent robots, 3D scene reconstruction and vision measurement. Such an issue is mainly caused by the distortion of camera [11] .

Existing solutions to the issue of camera distortion mainly focus on how to calibrate the camera [12,13,14,15]. These calibration techniques can improve the 3D depth information measurement problem caused by the distortion of camera to a certain extend. However, the performance of these methods is rather limited [16,17,18]. This mainly due they did not address the fundamental issue that the model of small hole imaging is appliable to the model of convex lens imaging the fundamental principle of small hole imaging is that light travels in a straight line after passing through the small hole. However, the lens of modern camera generally adopts a convex lens mode for condensing imaging [19,20].

Does the light that hits the optical center of convex lens propagate in a straight line? To answer this question, this paper studies the propagation mode of light passing through the convex lens. We first propose an angular affine transformation (AAT) model to realize expression of a simplified form of convex lens. Then, we propose a hypothesis that the propagation medium on both sides of simplified convex lens is homogeneous, but the medium on different sides is different (e.g., air on one side and convex lens material plus air on the other side). In the other words, the light entering the convex lens travels in a straight line. After entering the convex lens, it still travels in a straight line, but refraction will occur when the light passes through the convex lens. Based on the property that "the light rays, which are parallel to the main optical axis, will converge at the focal point when the pass through the simplified convex lens", we derive a calculation method of

[1]the College of Computer Science and Technology, ZheJiang University of Technology, ZheJiang, Hang Zhou , 310023, PR China

[2]the Department. of Computer Science, Hangzhou Normal University, Hangzhou, 311121, PR China. Corresponding Author: Jiafa Mao, E-Mail: maojiafa@zjut.edu.cn, and Weiguo Sheng, E-mail: w.sheng@ieee.org

the normal vector within the radius of convex lens. Finally, we study the propagation mode of light passing through the convex lens and address its propagation direction issue. The proposed theory has been verified using two sets of experiments: characterization of the route of light passing through the convex lens as well as camera imaging experiment. The experimental results are consistent with the phenomenon of light passing through the convex lens, which proves the validity of our theory. It can also be concluded that refraction will occurs after the light pass through the convex lens.

The rest of this paper is organized as follows: Section 2 give a general introduction to the propagation mode of light passing through convex lens. Section 3 studies the propagation mode of light entering the optical center. Section 4 investigates the propagation mode of light that neither enter the optical center nor parallel to the main optical axis. Experimental verification and summary are given in Section 5 and Section 6, respectively.

2. LPCL propagation modes in modern optics

Generally, when introducing convex lens in optics, the convex lens is denoted as "↕". Here, we will introduce three modes of propagation when light passes through a convex lens: 1) the propagation mode of the light rays hitting the optical center of convex lens (denoted as R_α), where α is the angle between the ray and main optical axis; 2) the light propagation mode parallel to the main optical axis (denoted as $R^{(x)}$), where x is the intersection point of the ray and "↕"; 3) a ray, which is neither hits the optical center nor parallel to the main optical axis (denoted as $R_\varphi^{(x)}$), where φ is the angle between the ray and main optical axis, and $\varphi \neq \alpha$ and x is the intersection of the ray and "↕". As shown in Figure 1, the red, blue, and green rays represent R_α, $R^{(x)}$, and $R_\varphi^{(x)}$, respectively.

In modern optics, the light ray directed to the optical center of convex lens does not change its direction when passing through the optical center, as shown by the red ray in Figure 1. When the rays, which are parallel to the main optical axis, are refracted by the convex lens, they will converge at the focal point of convex lens, as shown by the blue polyline in Figure 1. However, how the rest rays (such as rays, which are neither directed toward the optical center nor parallel to the main optical axis) will propagate after being refracted by the convex lens, how does the direction of refraction change? How much the change is? There is no such information in optics study.

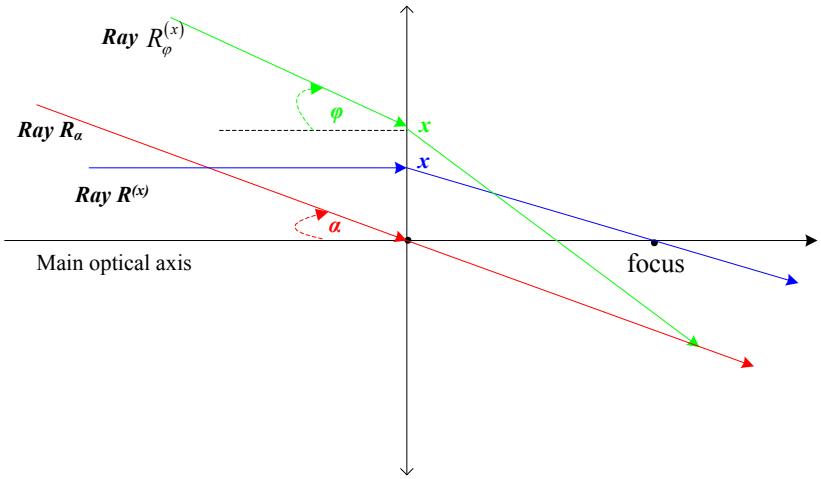

Figure 1. The diagram of optical path of convex lens in modern optics.

Will the LPCL travel in a straight line without being refracted? If this is true, then why the camera image will be distorted? What kind of refraction will happen to rays that are neither directed toward the optical center nor parallel to the main optical axis (as shown by the green broken line in Fig.1) after passing through the convex lens? What is the relationship between the angle of incidence and refraction? In the following sections, we will investigate these issues from two aspects: 1) the propagating mode of light entering the optical center; 2) the propagating mode of light, which is neither directed toward the optical center nor parallel to the main optical axis.

3.The mode of light propagation to the optical center of convex lens

In order to clarify the propagation mode of LPCL, we first restore the real optical path diagram.

3.1 The fundamental cause of distortion phenomenon of convex lens imaging

For the convenience of description, we will take the convex lens imaging as an example.

Suppose that the light-emitting point B emits a beam of ray R_α, under the condition of no refraction, the ray passing through the optical center O will intersect with image plane π_1 at B', as shown in red dashed line in Fig. 2. At the same time, suppose that the incident point of the ray R_α into the convex lens is B_1. Since the convex lens and air are different media, the ray R_α will inevitably undergo refraction. The ray R_α travels in a straight line in the convex lens and intersect with the convex lens at B_2. When the ray R exits from the convex lens, refraction will occur again. The intersection point of the emitted light to the image plane π_1 is B_3. The propagation path of the ray R_α is shown in red solid line in Fig. 2. At this time, B_3 is the real image of B. As the rays that are directed to the center of convex lens will travel in a straight line, which is consistent with the principle of pinhole imaging, the ideal image B' will not coincide with the real image B_3. While if the image is shifted, then the convex lens imaging is distorted, which is the fundamental reason of distortion phenomenon of camera imaging.

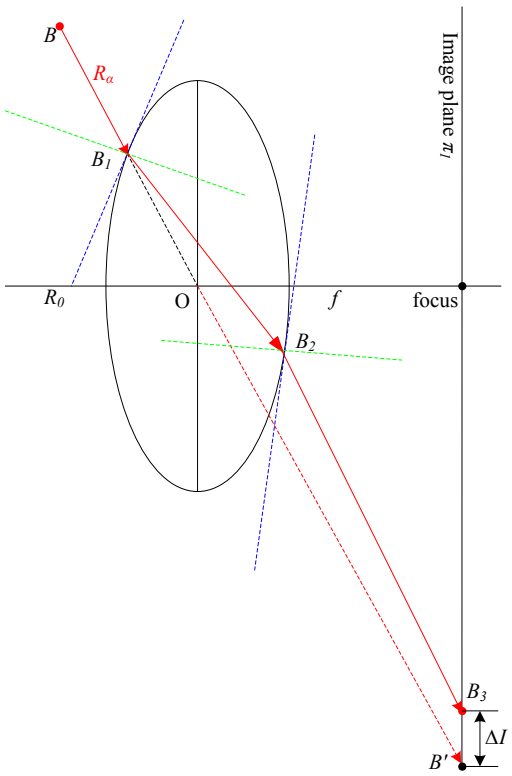

Figure 2. Diagram of the actual propagation route of the ray directed to the optical center.

3.2 Simplified processing of the propagation mode of light directed to the optical center of convex lens

To identify the offset of the ray (also called light vector) R_α passing through the optical center, from Figure 2, we can see that the material (or refractive index n) of convex lens as well as the contour curve function of convex lens needs to be known beforehand for solving the ray offset. However, the information about the materials of convex lens and its shape curve may not be available. While the focal length of convex lens of the camera can often be found in the image header file. This information might be used to solve the ray offset. For this purpose, we first simplify the mode of the light propagating towards the optical center.

First, we simplify the convex lens into a line segment, denoted as V_1V_2, which passes through the optical center O and is perpendicular to the main optical axis. The length of V_1V_2 is the diameter of convex lens ($2r$). Due to the symmetry of the upper and lower parts of convex lens, we only discuss the upper part OV_1 of convex lens, as shown in Figure 3.

How to represent the ray R_α, which is simplified into a line segment, after the convex lens? In other words, where should R_α fall on the straight-line segment OV_1? This is the key of simplifying the convex lens.

Suppose the angle between R_α and main optical axis to be α, we perform AAT on the ray angle α and the radius r of convex lens:

$$x = \frac{r}{\pi/2}\alpha, \alpha \in [0, \pi/2] \quad (1)$$

In above equation, when $\alpha = 0$ then $x = 0$ and when $\alpha = \pi/2$ then $x = r$. As the equation represents a uniform transformation, we call it angle-line uniform affine. Suppose a luminous point B emits a beam of ray R_α directed to the optical center, it intersects the optical center of cross-convex lens at the point O. After affine transformation by employing Eq. (1), its affine ray crosses OV_1 to x (that is α in the angular space). After the ray is refracted by convex lens, its propagation direction is shown in magenta dashed line in Figure 3.

In this section, we have simplified the propagation process of R_α. We can see that there is an offset problem when the light passes through the optical center. The next question is how to calculate the offset of the light passing through the optical center. This will be explained in the next section.

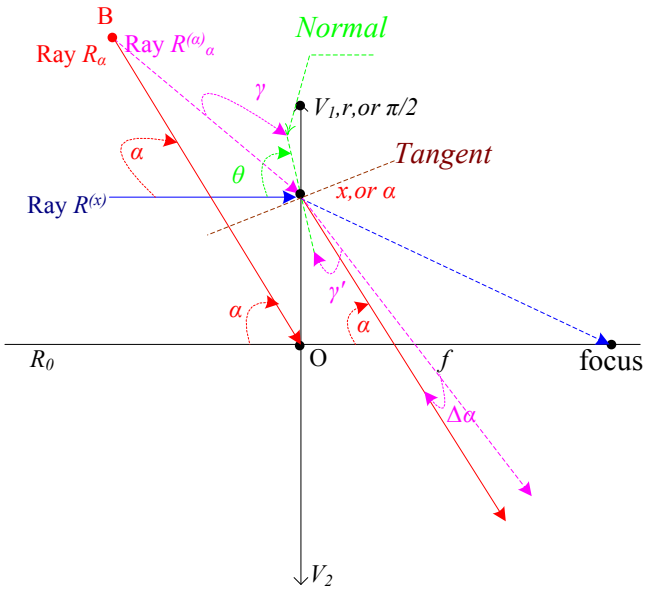

Fig. 3. The ray propagation process when the convex lens is simplified into a straight line.

3.3 Calculation method of ray $\mathbf{R_\alpha}$ offset

To calculate the offset of the ray passing through optical center, we must obtain two important parameters, the refractive index and the normal direction. In the following section, we should describe these in details.

3.3.1 The method of solving the refractive index of the medium on both sides of the convex lens

Assuming that the right side of convex lens is homogeneous (convex lens plus air), that is, the light travels in a straight line after passing through the convex lens. It is also assumed that the medium (air) between the light-emitting source and convex lens is also homogeneous, that is, the light also travels in a straight line from the light-emitting source to the convex lens, but the medium at two sides of the convex lens are different, as shown in Figure 4. Based on these assumptions, when the light passes from the left side of convex lens to the right side, its refractive index will not change. We denote its refractive index as n.

Also suppose the focal length of convex lens to be f. Since the convex lens has a light-gathering function, that is, the rays parallel to the main optical axis can converge at the focal point, it may be better to set the three rays parallel to the main optical axis as $R^{(x_1)}$, $R^{(x_3)}$ and $R^{(x_3)}$, where $R^{(x_1)}$ intersects the convex lens at the highest vertex.

Obviously, the tangent to the highest vertex of convex lens is parallel to the main optical axis, so the normal direction of this point must be perpendicular to the tangent. Since $R^{(x_1)}$ is parallel to the main optical axis and intersects with the convex lens at the highest vertex, then the incident angle of the ray $R^{(x_1)}$ (the angle between the incident light and the normal direction) is $\gamma = \pi/2$. Further, since the ray $R^{(x_1)}$ converges at the focal point after passing through the convex lens, its refraction angle (i.e., the angle between the refracted light and the normal direction) is $\beta = \tan^{-1}(f/r)$. Here $\tan^{-1}(\cdot)$ is the arctangent function, r is the radius of convex lens and $k = f/r$ denotes the focus ratio. Then, we can calculate the refractive index n between two sides of convex lens as:

$$n = \frac{\sin(\gamma)}{\sin(\beta)} = \frac{\sin(\pi/2)}{\sin(\tan^{-1}(f/r))} = \sec(\tan^{-1}(k)) \quad (2)$$

Why employ $R^{(x_1=r)}$ rays instead of $R^{(x_2)}$ or $R^{(x_3)}$ rays to calculate the refractive index n between the medium on both sides of the convex lens? The main reason is that our assumption is based on the propagation medium on both sides of the convex lens are homogeneous, the refractive index between the two mediums should be a fixed value. Also, the ray $R^{(x_2)}$ or $R^{(x_3)}$ is located within the radius r of convex lens, and its distance to the optical center of convex lens is uncertain, it is therefore impossible to obtain a fixed value of refractive index n. If the refractive index is not a constant value, then the propagation medium on both sides of the convex lens cannot be homogeneous, which contradicts our assumption.

Therefore, only the rays passing through the outermost end of the convex lens radius while parallel to the main optical axis can be used to calculate the refractive index between the propagation media on both sides of the convex lens.

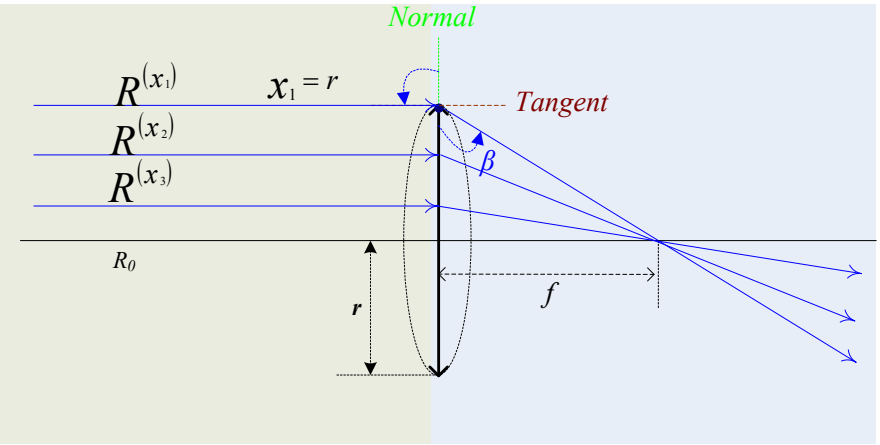

Figure 4. Light rays paralleling to the main optical axis converge at the focal point.

3.3.2 The method of solving the normal direction of ray R_α

According to the assumption in section 2.3.1: the left and right sides of convex lens line segment are two different but homogeneous medium. Then, we can obtain that the refractive index between the two medium is a constant. If the convex lens has a focusing function, then the normal direction within the line segment of convex lens can should be variable. How to calculate the normal direction (denoted as θ) of each point in line segment of convex lens? One approach is to employ the characteristic that the beam parallel to the main optical axis will converge to the focal point.

Suppose a beam of ray $R^{(x)}$ parallel to the main optical axis and it intersects the line segment OV_1 of cross-convex lens at x $(x \in [0, r]$, as shown in Figure 5. Suppose the incident angle γ of the ray $R^{(x)}$ is γ, and the refraction angle is β, then we can easily solve the relationship between them as:

$$\beta = \tan^{-1}\left(\frac{f}{x}\right) - \frac{\pi}{2} + \gamma \qquad (3)$$

Substituting formula (3) into formula (2), we can get:

$$\frac{\sin(\gamma)}{-\cos\left(\tan^{-1}\left(\frac{f}{x}\right)+\gamma\right)} = n \qquad (4)$$

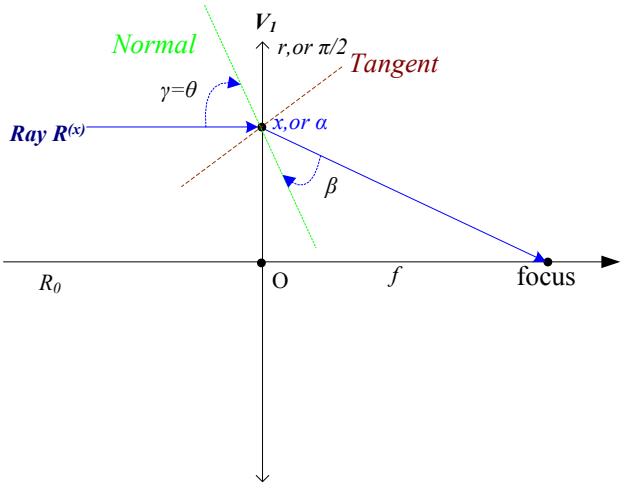

Figure 5. The calculation process of the normal direction of the ray R_α.

As shown in Fig.5, the incident angle γ at this time is exactly equal to the normal direction θ, that is, we can compute the normal direction θ as:

$$\theta = \tan^{-1}\left(\frac{n\cos(\rho)}{n\sin(\rho)-1}\right) \qquad (5)$$

Here, $\rho = \tan^{-1}(f/x) = \tan^{-1}\left(\pi f/(2r\alpha)\right)$ and n is the refractive index. It can be seen from Eqs. (3) and (5) that the normal vector θ of the ray R_0 is zero, then the light transmitted along the main optical axis will not deviate when passing through the optical center.

Fig. 6 shows the relationship between the incident angle α of the ray R_α and the normal vector θ of two camera types. The red solid line represents the focal length of the camera: $f = 50mm$, and the aperture value is $f/5.6$. The green solid line means the focal length of camera: $f = 4mm$, and the aperture value is $f/2.2$. When $\alpha \in [0, \frac{\pi}{2}]$, the red solid line will be always on the upside of the green solid line. That is, the larger the focal length, the larger the normal vector θ of ray R_α, and the normal vector θ of the ray R_α will be always larger than or equal to the incident angle α. Accordingly, based on the above analysis, we can obtain the relationship between the

normal direction and angle of incidence.

Property 1: When the incident angle $\alpha \in [0, \pi/2$ of the ray R_α directed to the optical center, the normal direction θ of convex lens will be always larger than or equal to the incident angle α, namely:

$$\theta \geq \alpha \qquad (6)$$

Proof is given in the appendix 1.

So far, we have solved the problem of calculation of normal direction.

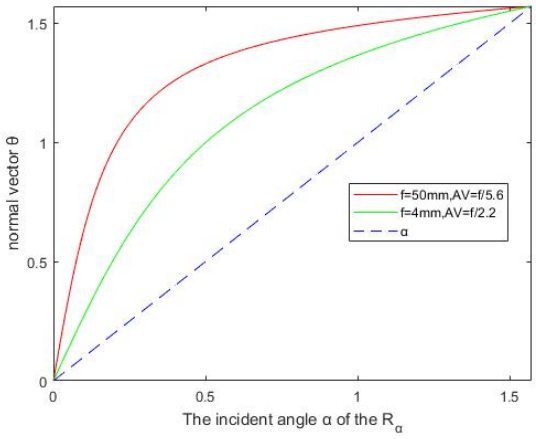

Figure 6. The relationship between the incident angle α of the ray R_α and the normal vector θ.

3.3.3 Calculation method of direction deviation of the ray R_α

As shown in Fig. 7, suppose a beam of light R_α, which has an angle α with the main optical axis, is directed to the optical center O of convex lens. From section 3.3, after simplifying the convex lens into a straight line, in the angular space, its entry point is α, $\alpha \in [0, \pi/2]$. That is, the ray R_α is translated upward by α units (in the line space, it means moving up $x(\alpha)$ units) and becomes the ray $R_\alpha^{(\alpha)}$. Also suppose that the normal direction at point α is θ, which can be obtained using Eq. (5). Then, the incident angle γ of the ray $R_\alpha^{(\alpha)}$ is:

$$\gamma = \theta - \alpha \qquad (7)$$

If the refraction angle of the ray $R_\alpha^{(\alpha)}$ is γ', employing the refractive index calculation method $\frac{\sin\gamma}{\sin\gamma'} = n$, we can obtain the refraction angle γ':

$$\gamma' = \sin^{-1}\left(\frac{\sin\gamma}{n}\right) \qquad (8)$$

Here, n is the refractive index and $\sin^{-1}(\cdot)$ is the inverse function of sine function. Also suppose the direction deviation of the ray$R_\alpha^{(\alpha)}$, after refraction, is $\Delta\alpha$, then it can be calculated as:

$$\Delta\alpha = \gamma - \gamma' = \theta - \alpha - \gamma' \qquad (9)$$

Here, θ and γ'' are all related to α. If α is known beforehand, then the direction deviation $\Delta\alpha$ of $R_\alpha^{(\alpha)}$, after refraction, can be calculated. Since $R_\alpha^{(\alpha)}$ is obtained by translating R_α upward by α, the direction deviation degree after R_α refraction is the same as the direction deviation degree $\Delta\alpha$ after $R_\alpha^{(\alpha)}$ refraction.

Fig.8 shows the direction offset of the ray R_α of the two types of camera lenses in Figure 6. The red solid line and green solid line are the offset $\Delta\alpha$ with the RFR $k = f/r$ of 5.6 and 2.2, respectively. Obviously, the blue solid color line is always above the solid red line. It can be seen from Fig. 8 that the larger the focal ratio k, the smaller the direction offset $\Delta\alpha$ of the ray R_α. Based on the above analysis, we can obtain the relationship between the RFR of convex lens k and the direction offset $\Delta\alpha$ of the rayR_α.

Property 2: Suppose the ratio of focal length to radius (RFR) of the convex lens as $k = f/r$, then the larger the value of k, the smaller the direction offset $\Delta\alpha$ of the rayR_α.

Proof is given in appendix 2.

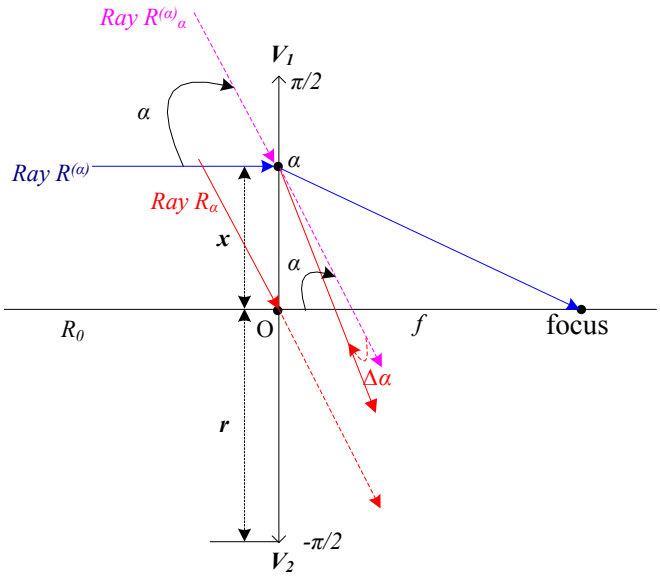

Figure 7. Diagram of the calculation method of offset of the rayR_α.

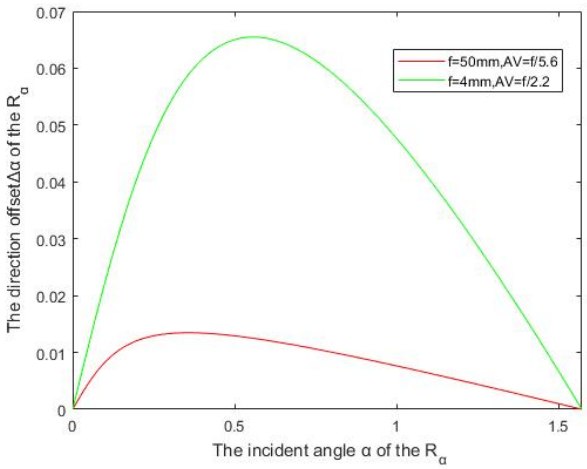

Figure 8. The direction offset of the ray R_α.

Property 2 shows that when employing the convex lens for imaging, the larger the focal ratio, the smaller the distortion and vice versa.

4. The light propagation mode of $R_{\varphi}^{(x)}(\varphi \neq \alpha)$

For the convenience of expression, we will express $R_{\varphi}^{(x)}$ as a ray that is neither directed to the optical center nor parallel to the main optical axis. In the line space, the incident point is at x and the intersection with the main optical axis at an angle φ. Obviously, when $x = x(\alpha), \varphi = \alpha$, the ray $R_{\alpha}^{(\alpha)}$ is the ray R_α moving upward or downward by α units.

As shown in Fig.9, when a beam of light ($R_{\varphi}^{(x)}$) that is neither directed toward the optical center nor parallel to the main optical axis, how to calculate the propagation direction τ of the light after passing through the convex lens? We derive the calculation method of τ as follows.

There are two situations: 1) when $\varphi \leq \theta(\alpha)$, that is, when the angle of incidence φ is less than or equal to the normal direction $\theta(\alpha)$ of the incident point α, that is, when $\varphi \leq \theta\left(\alpha = x^{-1}(\alpha)\right)$, the direction of light propagation; 2) when $\varphi > \theta(\alpha)$, that is, when the angle of incidence φ is larger than the normal direction $\theta(\alpha)$ of the incident point α, that is, when $\varphi > \theta\left(\alpha = x^{-1}(\alpha)\right)$, the direction of light propagation.

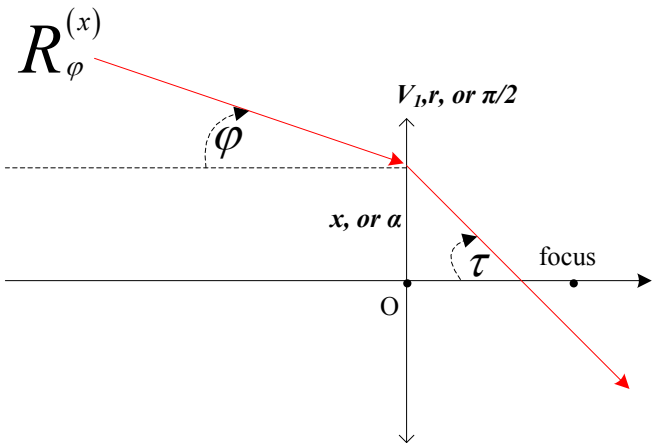

Figure 9. The propagation mode of light rays $R_{\varphi}^{(x)}$ that are neither directed to the optical center nor parallel to the main optical axis.

4.1 When the angle of incidence φ is less than or equal to the normal direction $\theta(\alpha)$ of the incident point α, the propagation direction of $R_{\varphi}^{(x(\alpha))}$

According to the property 1 in Section 2, the normal direction θ of the rayR_α directed to the optical center is always large than or equal to the incident angle α. Therefore, we can calculate the normal direction θ at the point $x = \alpha$ according to Eq. (5):

$$\theta = \theta(\alpha) \qquad (10)$$

Here, θ(·) is the normal direction function. Similarly, according to formula (8), the refraction angle γ' of the light can be calculated as:

$$\gamma' = \sin^{-1}\left(\frac{\sin(\theta(\alpha)-\varphi)}{n}\right) \qquad (11)$$

Then, the propagation direction τ of the light after passing through the convex lens can be calculated as:

$$\tau = \theta(\alpha) - \gamma' \qquad (12)$$

Here, $\alpha = x^{-1}(\alpha)$, $x^{-1}(\cdot)$ denotes the inverse function.

4.2 When the angle of incidence φ is large than the normal direction $\theta(\alpha)$ of the incident point α, the propagation direction of $R_{\varphi}^{(x(\alpha))}$

When a beam of light $R_{\varphi}^{(x(\alpha))}$ hits the convex lens, and the light satisfies the condition: when the angle of incidence φ is larger than the normal direction $\theta(\alpha)$ of the incident point α, then the incident angle of $R_{\varphi}^{(x(\alpha))}$ can be calculated as:

$$\gamma = \varphi - \theta(\alpha) \qquad (13)$$

The refraction angle γ' of $R_{\varphi}^{(x(\alpha))}$ can be written as:

$$\gamma' = \sin^{-1}\left(\frac{\sin(\varphi-\theta(\alpha))}{n}\right) \qquad (14)$$

Then, the propagation direction τ of the light after passing through the convex lens can be calculated as:

$$\tau = \theta(\alpha) + \gamma' \qquad (15)$$

Now, we can deduce the light propagation mode that is neither directed to the optical center nor parallel to the main optical axis.

5. Experimental verification

It is difficult to verify the propagation mode of rays passing through the convex lens without precise optical instruments. To alleviate this issue, a thorough verification scheme is required.

5.1 The design of the experiments

The rays passing through the convex lens from the luminous point B will be focused on the point B'. We can select three rays, the ray R_α that is directed to the optical center, one is higher than R_α and the other is lower than R_α, denoting as red, green, and blue rays in Figure 10(a). From the section 3.3.1 we know the rays before and after entering the convex lens and will propagate in a straight line. When the convex lens is simplified as a straight line, the optical path of the three rays can be found in in Figure 10(b).

We know that the generation of images mainly comes from cameras. The camera lens is a convex lens. Therefore, the camera imaging method should be used to verify our theory.

Based on the above analysis, we carry out two kinds of experiments to verify our theory: 1) delineation of the line passing through the convex lens ray. This can be carried out by employing MATLAB language to draw the light path diagram to check whether the light emitted from the luminous point will converge after passing through the convex lens; 2) camera imaging experiment. In these experiments, the light-emitting point will be photographed and imaged to see whether the image position is consistent with the actual image position.

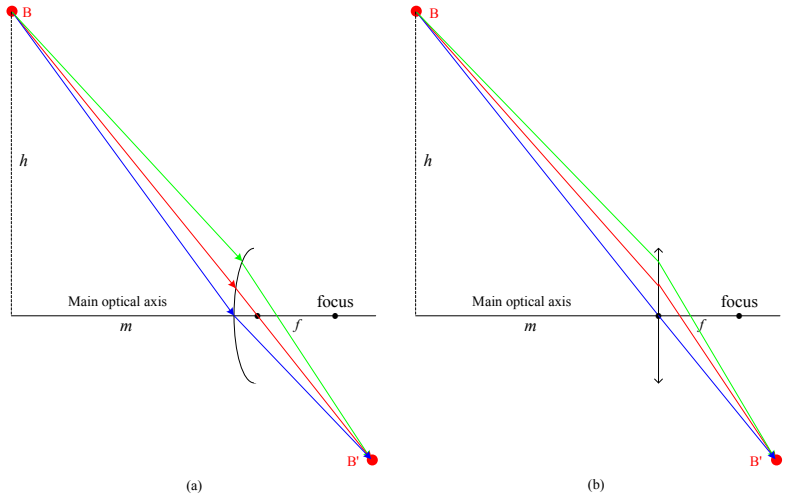

Figure 10. The light path diagram of light-emitting point B. The three rays in (a) are opposite to the three rays in (b).

5.2 LPCL experiments

5.2.1 Calculation method of virtual thickness of convex lens

Before the experiment, we should solve the problem of thickness of the incident point of convex lens. This is due to if this problem is not solved, it is difficult to calculate the angle α between the incident ray and the main optical axis.

It should be noted that the calculated convex lens thickness radius is not the actual convex lens thickness radius. This radius thickness is the virtual thickness produced by the mapping relationship between our angle and the convex lens radius. Therefore, we call d as the virtual thickness of convex lens.

Before the experiments, we should also solve the problem of the focal ratio of convex lens. This is due to, from Property 2, the RFR $k = f/r$ is directly related to the offset.

According to the literature 21, the focal length f of the convex lens is related to the thickness of convex lens, the refractive index of convex lens and the curve of the convex lens. The relationship between them can be written as:

$$f = \frac{n_1 r_1 r_2}{(n_1-1)(n_1(r_2-r_1)+(n_1-1)*d)} \qquad (16)$$

Here, the refractive index n_1 of the convex lens is related to the material of the convex lens. r_1 and r_2 are the radii of convex lens curve, respectively. d is the thickness of the convex lens. We suppose they are symmetrical, that is, $r_1 = r_2$. According to geometric properties, we can easily

calculate the relationship between the thickness of the convex lens d and the radius r_1 of convex lens curve as:

$$r_1 = r_2 = \frac{r^2+d_1^2}{2d_1} \quad (17)$$

Here, d_1 is half the thickness of the convex lens, that is, $d_1 = d/2$, and r is the radius of the convex lens. Substituting Eq. (17) into Eq. (16), we can obtain:

$$f = \frac{n_1(r^2+d_1^2)^2}{8d_1^3(n_1-1)^2} \quad (18)$$

Based on the relationship between the focal length of convex lens, the refractive index of the material of convex lens, the thickness of convex lens and the radius of convex lens, we then calculate the thickness of convex lens. Before doing so, we first introduce a theorem:

Theorem: Suppose the ray $R_\alpha^{(x(\alpha))}$ intersects the outer side of convex lens at B_1, the passing point B_1 is a parallel line parallel to the main optical axis and crosses OV_1 at B_2, and $x = |OB_2|$, then:

$$x = r\left(\frac{\pi}{2} - \alpha\right)\tan(\alpha), \alpha \in \left[0, \frac{\pi}{2}\right] \quad (19)$$

We call this Eq. (19) as parallel affine. See Appendix 3 for the proof.

According to the parallel affine theorem, then:

$$|B_1B_2| = \frac{x}{\tan(\alpha)} \quad (20)$$

Substituting Eq. (19) into Eq. (20), we get:

$$|B_1B_2| = r\left(\frac{\pi}{2} - \alpha\right) \quad (21)$$

Obviously, when $\alpha \to 0$, we can obtain the thickness radius of convex lens, d_1:

$$d_1 = \lim_{\alpha_1 \to 0}\left(r\left(\frac{\pi}{2} - \alpha\right)\right) = \frac{\pi r}{2} \quad (22)$$

It should be noted that Eq. (22) is not the true thickness of convex lens, but the virtual thickness obtained by affine transformation. Substituting Eq. (22) into formula (18), the RFR k can be calculated as:

$$k = \frac{f}{r} = \frac{n_1(1+(\pi/2)^2)^2}{\pi^3(n_1-1)^2} \quad (23)$$

Assuming that the refractive index of convex lens material is known, the RFR k of the convex lens can be calculated by employing Eq. (23). After solving the problem of the RFR of convex lens, we can then realize it to see if the luminous points converge to one point.

5.2.2 Experiment results

We regard the main optical axis of convex lens as X axis, the straight line perpendicular to the main optical axis as Y axis, and the optical center of convex lens as the origin of the coordinate system. Let's fix two rays first: 1) the ray R_α directed towards the optical center; 2) the ray $R_\varphi^{(0)}$ directed to the convex point on the left side of convex lens.

Then transform the third ray $R_\varphi^{(x(\alpha_1))}(0 < \alpha_1 \le \pi/2, and\ \alpha_1 \ne \alpha)$, that is, changing the incident point α_1 of the third ray. Let's check whether the three rays passing through the convex lens will converge and calculate the position information of the intersection of the two rays and the angle between the rays as well as the main optical axis.

We first carried out a set of experiments where the convex lens (focal length is 50mm) is made of quartz material, as shown in Figure 11 and Table 1. It can be seen from Figure 11 that when the luminous point emits a beam of rays directed to the convex lens, these rays will converge.

It can be seen from Table 1 that although the rays can converge, any three rays will not completely intersect at one point. It can be seen from the position information of the light-emitting points that the convergence points generated by the two light-emitting points at the same plane will not be located on the same plane. For example, the point (2500, 100) and the point (2500, 200) are in a plane perpendicular to the main optical axis 2500mm, but their convergence points are obviously not on the same plane perpendicular to the main optical axis. The luminous points (2500, 200) and (7500, 200) are located on a plane parallel to the main optical axis, but their converging positions are not on the same plane perpendicular to the main optical axis.

Table 1 The simulation results using the quartz convex lens ($n_1 = 1.48,\ f = 50$)

(m,h)(mm)	$\wedge(R_\alpha, R_\varphi^{(0)})$	α_i	$\wedge(R_\alpha, R_\varphi^{(x(\alpha_i))})$	$\wedge(R_\varphi^{(0)}, R_\varphi^{(x(\alpha_i))})$
(2500,100)	(51.0431, -1.8945)	$\alpha/3$	(51.1245, -1.8983)	(50.8812, -1.8885)
		$\alpha/2$	(51.1650, -1.9003)	(50.9218, -1.8900)
		$3\alpha/2$	(51.4064, -1.9116)	(51.1636, -1.8990)
		2α	(51.5256, -1.9173)	(51.2832, -1.9034)
(2500,200)	(51.3285, -3.8089)	$\alpha/3$	(51.6545, -3.8396)	(50.6886, -3.7615)
		$\alpha/2$	(51.8169, -3.8549)	(50.8492, -3.7734)
		$3\alpha/2$	(52.7771, -3.9452)	(51.8024, -3.8441)
		2α	(53.2452, -3.9893)	(52.2693, -3.8788)

(7500,200)	(50.3537, -1.2460)	$\alpha/3$	(50.3890, -1.2471)	(50.2833, -1.2443)
		$\alpha/2$	(50.4066, -1.2477)	(50.3009, -1.2447)
		$3\alpha/2$	(50.5120, -1.2510)	(50.4063, -1.2473)
		2α	(50.5644, -1.2527)	(50.4588, -1.2486)

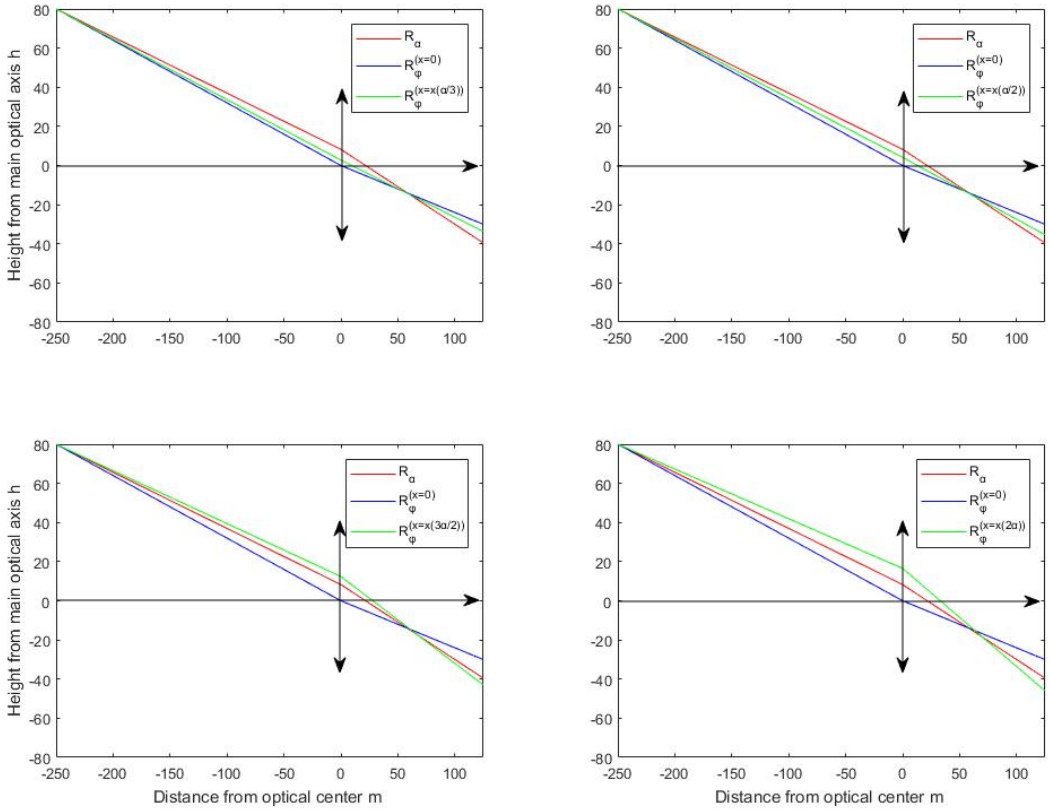

Fig.11 Experimental results of using a 50mm quartz convex lens with a focal length of 50mm. The coordinates of the luminous point are at (250, 80). $\alpha_i = \alpha/3, \alpha/2, 3\alpha/2, 2\alpha$ from top to bottom and from left to right, respectively.

We also carried out a set of experiments with heavy flint glass (with a focal length of 50mm) as the material. The experimental results are shown in Table 2, which is similar to the results in Table 1. Comparing the results in Table 1 and Table 2, we can see that the larger the refractive index of convex lens material, the better the convergence. Based on the same luminous point (for example, the coordinates are (7500, 200)), the rays will converge near 1.2460 from the main optical axis for Quartz and near 1.0272 for heavy flint glass.

T

able 2 Simulation results using heavy flint glass ($n_1 = 1.75496, \quad f = 500$)

(m,h)(mm)	$\Lambda\left(R_\alpha, R_\varphi^{(0)}\right)$	α_i	$\Lambda\left(R_\alpha, R_\varphi^{(x(\alpha_i))}\right)$	$\Lambda\left(R_\varphi^{(0)}, R_\varphi^{(x(\alpha_i))}\right)$
(2500,100)	(50.7684, -1.5563)	$\alpha/3$	(50.8000, -1.5579)	(50.7055, -1.5544)
		$\alpha/2$	(50.8157, -1.5587)	(50.7213, -1.5548)
		$3\alpha/2$	(50.9084, -1.5635)	(50.8150, -1.5577)
		2α	(50.9537, -1.5659)	(50.8609, -1.5591)
(2500,200)	(50.7367, -3.1076)	$\alpha/3$	(50.8622, -3.1205)	(50.4876, -3.0923)
		$\alpha/2$	(50.9245, -3.1269)	(50.5503, -3.0962)
		$3\alpha/2$	(51.2903, -3.1647)	(50.9199, -3.1188)
		2α	(51.4665, -3.1829)	(51.0990, -3.1298)
(7500,200)	(50.2524, -1.0272)	$\alpha/3$	(50.2660, -1.0276)	(50.2250, -1.0266)

$\alpha/2$	(50.2728, -1.0279)	(50.2319, -1.0268)
$3\alpha/2$	(50.3135, -1.0293)	(50.2727, -1.0276)
2α	(50.3337, -1.0300)	(50.2930, -1.0280)

5.3 Camera imaging experiments

The camera imaging experiment is used to verify correctness of our proposed theory. The experiments are carried out as follows: taking the light-emitting point and image it, and calculate whether the image position is consistent with the actual image position.

5.3.1 Experimental method design

When the camera's focus and image distance are accurate, it will be able to produce a clear image point of the light-emitting point on camera's photosensitive element. However, we typically have no idea of the material of convex lens. In this case, the refractive index and focal ratio of the convex lens cannot be calculated by the method in section 5.2.1. So how to carry out camera imaging experiments to prove our theory?

Fortunately, the header file of image taken by the camera contains the image resolution, focal length, aperture value, maximum aperture, and other parameters. Therefore, we can use this information to obtain the key parameter, RFR.

Therefore, the following experimental scheme has been carried out.

We paste 11 red solid circles on a white wall, each circle is given a number, A, B, C, D, E, F, G, H, I, J, K, respectively, as shown in Figure 12. Among them, circle A is a reference point, and the relative positions of other points to circle A are shown in Table 3. By facing the circle distribution map and letting the main optical axis of the camera to be aligned with the center of circle A, we then take pictures to obtain red solid circles.

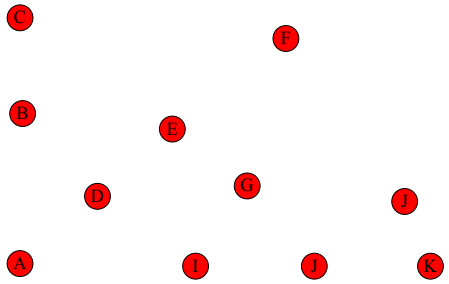

Figure 12. The distribution map of target points.

By performing digital-to-analog conversion to obtain the distance from each point to the image center, then, by employing our proposed method to obtain the distance between these points and the image center to see if the data obtained by the two methods are consistent.

Table 3 Distribution of experimental data relative to circle A

Point	B	C	D	E	F	G	H	I	J	K
Distance from A(mm)	197.1	328.9	128.4	274.1	452.6	311.7	501.2	237.3	378.7	525.0

5.3.2 Experimental results

The camera of Huawei Honor is employed. The parameters of image obtained by the shooting are: focal length 4mm, 35mm, focal length 27mm, aperture value *f/2.2* and resolution 5120*3840. The images are taken at distances from circle A of 1784, 2701, 3872, 4369, 5353mm, respectively. When shooting, we first take a set of images at a distance of 3872 mm from the camera. When shooting, we point the main optical axis to the circle. In the other word, let the circle A to be located at the center of the image. The HoughCircles segmentation algorithm [22] is employed for segmentation. The results are shown in the third column of Table 4. The fourth column in Table 4 is the calculation method of the distance from point A obtained by digital-to-analog conversion as follows:

$$ds = \sqrt{\left(\frac{X-X_A}{M} * w\right)^2 + \left(\frac{Y-Y_A}{N} * l\right)^2} \qquad (24)$$

Here, , $M \times N$ is the image resolution, $w \times l$ is the size of photosensitive element, (X_A, Y_A) is the coordinate of point A and (X, Y) is the coordinate of the point to be calculated.

It can be seen from Table 4 that the values of ds column are very close to the value of the $R_\varphi^{(0)}$ column, and the average correlation is 0.032487mm. By converting it into pixels, it is about 6 pixels (0.006mm/pixel). The value in ds column is relatively larger than the value in R_α column. The average difference is 0.04626mm (approximately 7.71 pixels). If the ray $R_\varphi^{(0)}$ is selected as the imaging light of the camera, its value is almost consistent with those calculated by our proposed theory.

To further verify our theory, we took four sets of target images, the distances are 1784, 2701, 4369, 5353mm, respectively. The experimental results are shown in Fig.13. It can be seen from FIG. 13 that in either case, the value of the ds column is always very close to the value of $R_\varphi^{(0)}$ column, and the difference is less than 10 pixels. This

further illustrates the correctness of our theory.

Table 4 Experimental results based on Huawei Honor camera

M(mm)	points	HoughCircles [22]		ds (mm)	Ours method	
		X(pixel)	Y(pixel)		$R_{\varphi}^{(0)}$	R_{α}
3872	B	2312	1826	1.284	1.2752	1.2662
	C	2312	1686	2.124	2.1273	2.1095
	D	2408	1938	0.8404	0.8308	0.8253
	E	2518	1830	1.765	1.7731	1.7594
	F	2652	1692	2.9191	2.9260	2.8965
	G	2618	1900	2.019	2.0161	1.9997
	H	2838	1818	3.4256	3.2395	3.2043
	I	2552	2038	1.44	1.5352	1.5238
	J	2720	2036	2.4481	2.4490	2.4269
	K	2878	2036	3.3961	3.3930	3.3547

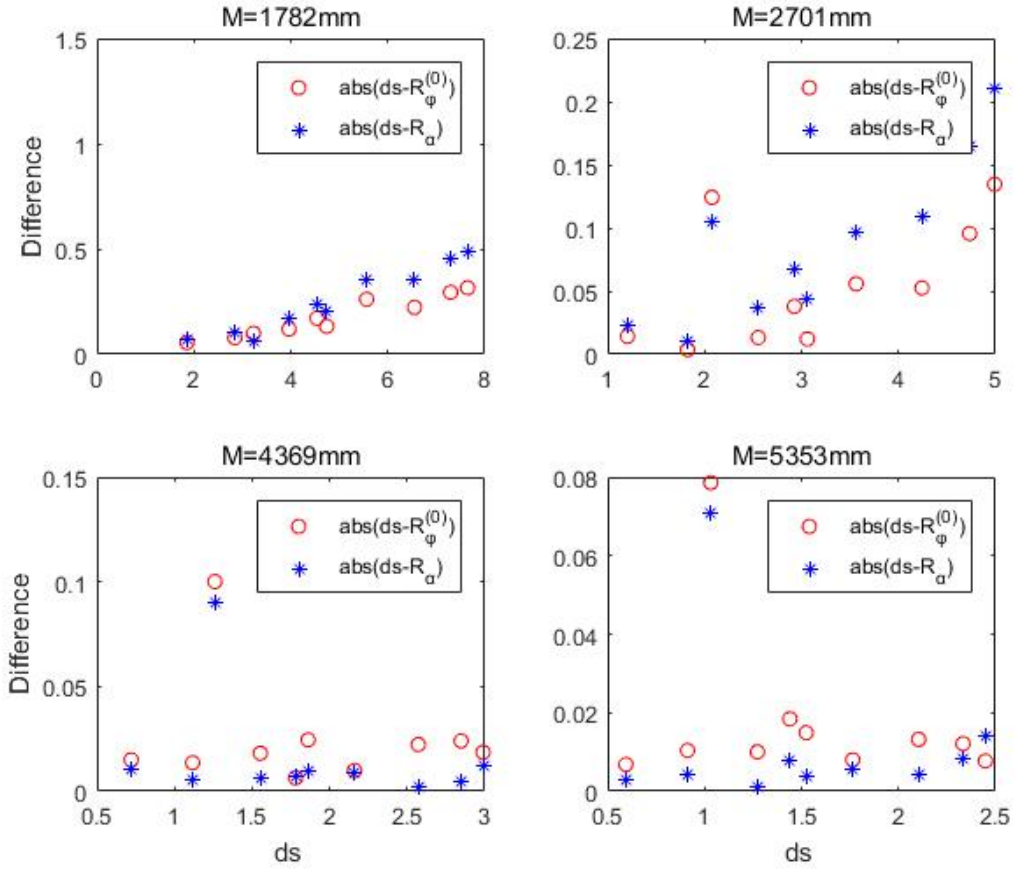

Figure 13. Experimental results where the distance between the target and camera at 1784, 2701, 4369, 5353mm, respectively

5.4 Analysis, discussion, and comparison

5.4.1 Analysis and discussion

It can be seen from Tables 1 and 2 that any luminous point emits three rays directed to the convex lens. After they are refracted by the convex lens, these rays do not intersect at one point, but each two of them will intersect to obtain three intersection points. Although these three intersection points are very close to each other, they are not converging at one point. Therefore, if a baffle is placed on the other side of convex lens and is perpendicular to the main optical axis, then no matter how far the baffle is from the convex lens, it is impossible to form one light point.

For example, assuming that the position of the baffle

is at the focal point of convex lens and the position of light-emitting point is (7500,200). We calculate three rays R_α, $R_\varphi^{(0)}$, $R_\varphi^{(x(\alpha/3))}$ separately. After being refracted by the convex lens, it is obvious that $\alpha = \tan^{-1}(200/7500) = 0.0267$. The three intersection points will be at (50.3537, -1.2460), (50.2660, -1.0276) and (50.2250, -1.0266), respectively. Although these three points are very close, they are not the same. Considering only that the incident angle of rays is in the range of $[0, \alpha]$, these rays can form a spot. This is the same as the situation described in the principle of convex lens imaging, and it also shows the correctness of our theory.

Tables 1 and 2 show when a luminous point emits a beam of rays to the convex lens, only one spot can be formed, not one point. If the light entrance aperture of convex lens is controlled, (i.e., controlling the light entrance quantity), then the diameter of light spot can be reduced. When the diameter of the light spot tends to zero, then a light point is formed. This is consistent with the camera principle, and further illustrates the correctness of our theory.

It can be seen from Table 4 and Figure 13 that although the value of ds is very close to the value of *, there is a certain error, and the largest error is nearly 10 pixels. Technically, there should be no error. So why the error exists? The reasons are summarized as follows.

1) Shooting error. This is mainly caused by using Huawei mobile phone as the experimental camera, which does not have the light matching function. Although we try to precisely locate the center point of circle A (i.e., reference point) during the shooting process, it is generally difficult to make the main optical axis to be completely aligned with the reference point.

Certainly, professional cameras could be employed for experiments. However, these cameras generally consist of multiple lens including concave lens and convex lenses to prevent deforming. For example, one Nikon camera could have 6 lenses. So, they cannot meet our experimental requirements.

2) Measurement error. A laser pointer has been used to measure the distance between the target and camera. Due to operational reasons, a small amount of measurement error may occur.

3) Segmentation error. The HoughCircles algorithm [22] has been employed for segmentation. This method has been widely used segmentation of circular targets and a certain deviation of the segmentation results is inevitable.

It should be noted that these deviations will generally not affect our theory in real applications. For example, to apply our theory for camera distortion corrections, it does not require to consider the reference point in the distortion correction.

Based on above analysis and discussion, it is clear that the ray $R_\varphi^{(0)}$ directed to the most convex point of convex lens. After affine transformation, it will hit the optical center. The ray R_α is originally a ray directed to the optical center of convex lens. After affine transformation, it is not the ray directed to the optical center. It can also be seen from Table 4 and Figure 13 that the difference between ds and $R_\varphi^{(0)}$ is smaller than the difference between ds and R_α. Therefore, the phantom ray $R_\varphi^{(0)}$ is actually the ray hitting the optical center after affine transformation when the convex lens is simplified into a straight line. This ray is also refracted after passing through the optical center.

It therefore further illustrates our theory: the rays (except the main optical axis) directed to the optical center of convex lens will be refracted. The widely accepted statement: "the rays directed to the optical center of the convex lens propagate along a straight line" is not true.

5.4.2 Experimental comparisons

People may wonder why use uniform affine instead of parallel affine? To classify this problem, experiments have been performanced to compare the difference of using uniform affine and parallel affine. The experiments are carried out using Huawei Honor camera with the target distance to be 3972mm.

Fig. 14 shows the experimental results when the radius of convex lens is set to be r=20mm, in which the green straight line represents uniform affine, while the blue curve is parallel affine. The difference between the two lines is denoted using a red dashed line. In the range of angle $\alpha \in [0.\pi/2]$, the length in the line space obtained after parallel affine is always greater than or equal to the length obtained after uniform affine, and the maximum difference is 5.7575mm ($\alpha = 0.7069$). From the results, we can see that by employing the parallel affine method to simulate the point-of-light imaging, the diameter of generated light spot will be larger than that generated by uniform affine. Therefore, uniform affine could have a better performance than parallel affine.

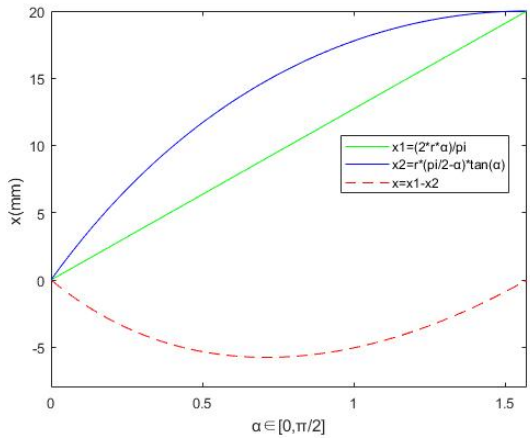

Figure 14. The difference between uniform affine and parallel affine.

We compared the uniform affine and parallel affine at 5353mm from the camera to light-emitting point. The results are shown in Table 5. It can be seen from Table 5 that the distance between the intersection of uniformly affine R_α and the focal plane is always closer to the center of the image than the parallel affine. However, the distance of intersection point of their rays $R_\varphi^{(0)}$ and focal plane is far away to the center of image is exactly the same, which is very close to the distance between the luminous point and the center of image (refer to the second column of Table 5). Based on the results, we can see that if using the $R_\varphi^{(0)}$ line to perform the camera distortion correction, the correction performance is the same regardless the affine method used. We also calculated the distance between the intersection of the straight line passing through the optical center and focal plane from image center (refer to the third column of Table 5) when refraction does not occur (that is, the principle of pinhole imaging). Comparing the results reported in columns 4 to 7 in Table 5, we can see that the distance traveled in a straight line is larger than other values. If the photosensitive element of the camera is placed on the focal plane, the distortion will make the image becoming smaller.

Table 5 Comparison the results of employing uniform affine and parallel affine

Points	ds(mm)	Pinhole imaging	Uniform affine		Parallel affine	
			$R_\varphi^{(0)}$	R_α	$R_\varphi^{(0)}$	R_α
B	0.9121	0.9942	0.9225	0.9164	0.9225	0.9177
C	1.5242	1.6589	1.5391	1.5278	1.5391	1.5193
D	0.5942	0.6476	0.6010	0.5971	0.6010	0.5995
E	1.2728	1.3825	1.2828	1.2738	1.2828	1.2708
F	2.1043	2.2829	2.1175	2.0999	2.1175	2.0700
G	1.4402	1.5722	1.4586	1.4481	1.4586	1.4416
H	2.3325	2.5280	2.3446	2.3241	2.3446	2.2821
I	1.032	1.1969	1.1106	1.1030	1.1106	1.1026
J	1.764	1.9101	1.7720	1.7584	1.7720	1.7428
K	2.4481	2.6480	2.4558	2.4338	2.4558	2.3850

The above two sets of experiments reveal that the condensing performance of uniform affine is better than that of the parallel affine. When the aperture of convex lens is small enough for imaging, such as the ray $R_\varphi^{(0)}$ can pass through, then both types of affine modes can solve the distortion problem of camera.

6. Conclusions

In optics research, rays passing through the optical center of convex lens will travel in a straight line is deemed to be a fundamental theory. This concept is consistent with the pinhole imaging theory, which is used to characterize camera imaging model. However, based on such a theoretical framework, applications such as engineering measurement, 3D reconstruction and visual navigation are often seriously affected by camera distortion, leading to large errors. Although, this phenomenon has been received attention, there is no theoretical explanation available for these errors.

In this paper, we investigate the propagation mode of light passing through convex lens. Specifically, assuming the propagation medium on both sides of convex lens is homogeneous, we propose an angular affine transformation theory. Based on the proposed theory, we first derive the refractive index of convex lens as well as the method of calculating the normal direction of each point within the radius of convex lens radius and then derive the refraction direction of each point within the radius of convex lens, thus completely characterizing the path diagram of light directed to the optical center. Two

kinds of experiments (i.e., experiments of light passing through the convex lens and the camera imaging experiments) have been carried to confirm the correctness of our proposed theory. The results reveal that the fundamental theory of optics research (i.e., the light rays hitting the optical center of convex lens propagate in a straight line) is not correct.

The results of this article will provide a theoretical basis for the camera distortion correction and will also change the theoretical framework of the pinhole imaging model. Employing the proposed theory, we will carry out research on engineering applications such as 3D reconstruction, target depth measurement, and visual navigation. We will mainly focus on the 6-DOF (x y z yaw pitch roll) information measurement method of the target in a single image and provide technical support for monocular vision navigation technology.

Acknowledgments: This work is supported by National Natural Science Foundation of China (Nos. 62176237,61873082), the ZheJiang province Natural Science Foundation of China (No. LY20F020022).

References

1. Karnieli A., Trajtenberg-Mills S., and Arie, A., Observation of the nonreciprocal adiabatic geometric phase in nonlinear optics. 2019 Conference on Lasers and Electro-Optics (CLEO). pp. 2-3, San Jose, CA, USA, 5-10,(2019).

2. Snyder AW, Mitchell DJ, and Kivshar YS, Unification of Linear and Nonlinear-Wave Optics, Modern Physics Letters B. Vol.9, No.23, pp.1479-1506, (1995).

3. Agnew M., Bolduc E., Boyd R.W., et al. New Results in Quantum Nonlinear Optics. pp.469-502, 2012 IEEE Photonics Conference(IPC), Burlingame, CA. SEP 23-27, (2012).

4. Schmidt B.E., Lassonde P., Ernotte G. ,et al, Linearizing Nonlinear Optics. 21st International Conference on Ultrafast Phenomena (UP). Vol.205, pp.1-3, Hamburg, GERMANY, JUL 15-20, (2018).

5. Jia Ping, Analysis on present development status and future prospect of some precision instruments and equipment in China, Science & Technology Review, Vol.35, No.11, pp.39-46, (2017).

6. Lv Wenjun, Kang Yu, Zhao Yun-Bo."FVC: A Novel Nonmagnetic Compass." IEEE Transactions on Industrial Electronics,Vol.66, No.10, pp.7810-7820, (2019).

7. Ding Peng, Zhang Ye, Jia Ping, et al, Ship Detection on Sea Surface Based on Visual Saliency. Acta Electronica Sinica. Vol.48, No.1, pp.127-134, (2018).

8. Shervin Shirmohammadi and Alessandro Ferrero. "Camera as the Instrument: The Rising Trend of Vision Based Measurement.", IEEE Instrumentation and Measurement Magazine, Vol.17, No. 3, pp. 41-47. (2014)

9. Charalampous K, Kostavelis I, Gasteratos A. ."Thorough robot navigation based on SVM local planning." Robotics & Autonomous Systems, Vol.70, pp.166-180, (2015).

10. Wang H . ,Zhao, J., Zhao JW et.al, A New Rapid-Precision Position Measurement Method for a Linear Motor Mover Based on a 1-D EPCA, IEEE Trans. on Industrial Electronics. Vol.65, No.9, pp.7485-7494. (2018).

11. Jia T, Shi Y, Zhou Z X, et al. 3D depth information extraction with omni-directional camera. Information Processing Letters,,Vol. 115, No.2,pp.285-291. (2015).

12. A bdel-A ziz YI, Karara HM. Direct linear transformation into object space coordinates in Close-Range Photogrammetry. ProcSymp. Close-Range Photogrammetry. 1-18,(1971).

13. Tsai. A versatile camera calibration technique for high-accuracy 3D machine vision metrology using off-the-shelf TV cameras and lenses. IEEE Journal of robotics and automation, Vol. RA-3(4):323-344,(1987).

14. Z.Zhang, Flexible camera calibration by viewing a plane from unknown orientations. Proceedings of the 7th International Conference on Computer Vision, 666-673,(1999).

15. Zhang ZY. Camera calibration with one-dimensional objects. IEEE Transactions Pattern Analysis and Machine Intelligence, 26(7):892- 899,(2004).

16. M. Pollefeys. R. Koch and L. Van Gool, Self-calibration and metric reconstruction in spite of varying and unknown internal camera parameters[C]. Proceedings of the 6th International Conference on Computer Vision, 90-95, (1998).

17. Ferran Espuny. A new linear method for camera self-calibration with planar motion[J]. Mathematical Imaging and Vision, 2007: 81-88.

[18] Lee Chang-Ryeo, Yoon, Kuk-Jin,. "Confidence analysis of feature points for visual-inertial odometry of urban vehicles. " IET Intelligent Transport Systems , Vol.13, No.7, pp.1130-1138,(2019).

19. Xu Dan, Ricci Elise, Ouyang Wanli, Wang Xiaogang, Sebe Nicu."Monocular Depth Estimation Using Multi-Scale Continuous CRFs as Sequential Deep Networks." IEEE Transactions on Pattern Analysis and Machine Intelligence, Vol.41, No.6, pp1426-1440. (2019).

20. Cheng Guo, Meng Xiao, Meir Orenstein & Shanhui Fan, Structured 3D linear space–time light bullets by nonlocal nanophotonics, Light: Science & Applications(2021) 10:160. pp.1-16,(2021).

21. Yao Qijun, Optical Course (Sixth Edition), Higher Education Press, 03, (2009).

22. D. H . BALLARD. Generalizing the Transform to Detect Arbitrary Shapes. Pattern Recognition. Vol.13, No.2, pp.111-122. (1981).

Appendix 1

Proof: Let the unary function $\Phi(\alpha) = \theta - \alpha$ and substitute Eq. (5) into $\Phi(\alpha)$ to obtain:

$$\Phi(\alpha) = \tan^{-1}\left(\frac{n\cos(\rho)}{n\sin(\rho)-1}\right) - \alpha =$$

$$\tan^{-1}\left(\frac{n\cos(\tan^{-1}(f\pi/(2r\alpha)))}{n\sin(\tan^{-1}(f\pi/(2r\alpha)))-1}\right) - \alpha \qquad (1\text{-}1)$$

When $\alpha = 0$, $\tan^{-1}(f\pi/(2r\alpha)) = \tan^{-1}(+\infty) = \pi/2$, therefore $\Phi(0) = 0$. When $\alpha = \pi/2$, $n\sin(\rho) - 1 = n\sin(\tan^{-1}(f/r)) - 1$ and $n = \sec(\tan^{-1}(f/r))$, therefore, $n\sin(\rho) - 1 = 0$, that is, $\Phi(\pi/2) = \tan^{-1}(+\infty) - \pi/2 = 0$. Therefore:

$$\Phi(0) = \Phi(\pi/2) = 0 \qquad (1\text{-}2)$$

Let $\rho = \tan^{-1}(f\pi/(2r\alpha))$, denote the function $\psi(\alpha)$ as:

$$\psi(\alpha) = \tan(\theta) = \frac{n\cos(\rho)}{n\sin(\rho)-1} \qquad (1\text{-}3)$$

Deriving the equation (1-3) with respect to α, we can obtain:

$$\frac{d\psi}{d\alpha} = \frac{2nf\pi r(n-\sin(\rho))}{(4r^2\alpha^2+f^2\pi^2)(n\sin(\rho)-1)^2} \qquad (1\text{-}4)$$

It can be seen from the Eq. (1-4) that the numerator is always greater than zero and the denominator is always greater than zero, so the formula (1-4) is always greater than zero. Here we can see the function $\psi(\alpha)$ in $\alpha \in (0, \pi/2)$ /2) is monotonically increasing. By deriving the equation (1-4) against α, we have:

$$\frac{d^2\psi}{d\alpha^2} = \frac{2nf\pi r^2}{(n\sin(\rho)-1)^2(4r^2\alpha^2+f^2\pi^2)} * \left(-2f\pi\cos(\rho) - 8r\alpha - \frac{4nf\pi\cos(\rho)(n-\sin(\rho))}{n\sin(\rho)-1}\right) \qquad (1\text{-}5)$$

Since when $\alpha \in (0, \pi/2)$, then $\rho \in (\tan^{-1}(f/r), \pi/2)$, $\cos(\rho) > 0$. $n\sin(\rho) - 1$ is a monotonically decreasing function with respect to α, and when $\alpha = \pi/2$, $n\sin(\rho) - 1 = 0$, that is, when $\alpha \in (0, \pi/2)$, $n\sin(\rho) - 1 > 0$, therefore, we can get:

$$\frac{d^2\psi}{d\alpha^2} < 0, \alpha \in (0, \pi/2) \qquad (1\text{-}6)$$

From equations (1-3), we can get:

$$\theta = \tan^{-1}(\psi(\alpha)) \qquad (1\text{-}7)$$

The second derivative of equation (1-7) can be obtained as:

$$\frac{d^2\theta}{d\alpha^2} = \frac{\frac{d^2\psi}{d\alpha^2}(1+\psi^2(\alpha)) - 2\psi(\alpha)\frac{d\psi}{d\alpha}}{(1+\psi^2(\alpha))^2} \qquad (1\text{-}8)$$

From equation (1-6), $\frac{d^2\psi}{d\alpha^2} < 0$, from equation (1-4), $\psi(\alpha)\frac{d\psi}{d\alpha} > 0$, so:

$$\frac{d^2\theta}{d\alpha^2} < 0, \alpha \in (0, \pi/2) \qquad (1\text{-}9)$$

Because $\frac{d^2\Phi}{d\alpha^2} = \frac{d^2\theta}{d\alpha^2}$, therefore, $\Phi(\alpha)$ is a convex function in the range of $\alpha \in (0, \pi/2)$, Combining Eq. (1-2), we can get:

$$\Phi(\alpha) = \theta - \alpha \geq 0, \alpha \in [0, \pi/2] \qquad (1\text{-}10)$$

That is, $\theta \geq \alpha$.

End proof.

Appendix 2

Proof: To prove that property 2, we need to prove that the direction offset Δα is a monotonically decreasing function with respect to RFR k=f/r. We denote the function of direction offset on the RFR to be $\tau(k)$, then we only need to prove that $\tau(k)$ is a monotonically decreasing function.

Substituting k=f/r into Eq. (10), we get:

$$\tau(k) = \gamma(k) - \beta(k) \qquad (2\text{-}1)$$

The Eq. (6) can also be expressed as:

$$\rho(k) = \tan^{-1}\left(k/\left(\left(\frac{\pi}{2} - \alpha\right)\tan(\alpha)\right)\right) \qquad (2\text{-}2)$$

Obviously, when $\alpha \in [0, \pi/2]$, $\rho \in [\tan^{-1} k, \pi/2]$. Let $x = (\pi/2 - \alpha)\tan(\alpha)$, then Eq. (2-2) can be simplified as:

$$\rho(k) = \tan^{-1}(k/x) \qquad (2\text{-}3)$$

By deriving equation (2-3) with respect to k, we can obtain:

$$\frac{d\rho}{dk} = \frac{1}{1+(k/x)^2} \qquad (2\text{-}4)$$

Obviously $\frac{d\rho}{dk} > 0$ holds. We take the derivative of k on both sides of Eq. (5) and get:

$$\frac{d\theta}{dk} = \frac{1}{1+\left(\frac{n\cos\rho}{n\sin\rho-1}\right)^2} * \frac{-n\sin\rho - n(n-\cos\rho)}{(n\sin\rho-1)^2} * \frac{d\rho}{dk} \qquad (2\text{-}5)$$

Since the refractive index $n > 1$ and $\cos\rho < 1$, we can easily reach a conclusion that $\frac{d\theta}{dk} < 0$. From the Eq. (8), we can get:

$$\frac{d\gamma}{dk} = \frac{d\theta}{dk} < 0 \qquad (2\text{-}6)$$

We take the derivative of k in the main text of equation (10) and get:

$$\frac{d\beta}{dk} = \frac{1}{\sqrt{1-(\sin\gamma/n)^2}} * \frac{\cos\gamma}{n} * \frac{d\gamma}{dk} \qquad (2\text{-}7)$$

Since $\frac{1}{\sqrt{1-(\sin\gamma/n)^2}} < 1$, $\frac{\cos\gamma}{n} < 1$, we have:

$$\begin{cases} \frac{d\beta}{dk} < 0 \\ \left|\frac{d\beta}{dk}\right| < \left|\frac{d\gamma}{dk}\right| \end{cases} \qquad (2\text{-}8)$$

From the above steps, we can get:

$$\frac{d\tau}{dk} = \frac{d\gamma}{dk} - \frac{d\gamma'}{dk} < 0 \qquad (2\text{-}9)$$

Finally, we can conclude that the offset $\Delta\alpha$ is a monotonically decreasing function with respect to the RFR k. In the other words, the property 2 holds.

End Proof.

Appendix 3

Proof: As shown in Fig.1 of Appendix. Suppose the distance from point B_1 to the main optical axis is x, $|B_1B_2| = d$. Then:

$$x = \mathrm{d} * \tan(\alpha) \qquad (3\text{-}1)$$

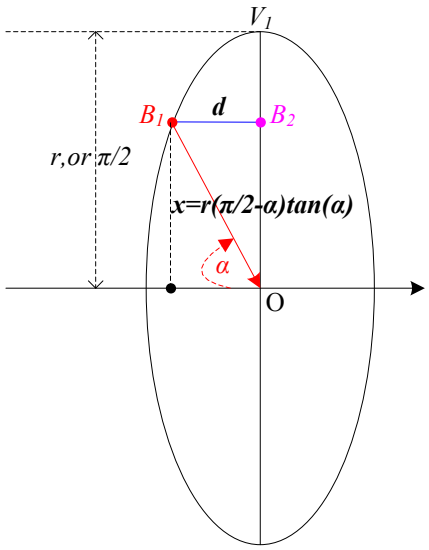

Figure 1 of Appendix. The relationship between firing angle α and $|OB_2|$

We know that when $\alpha \to \pi/2$ and $x \to r$, then:

$$\lim_{\alpha\to\pi/2} \mathrm{d} * \tan(\alpha) = \lim_{\alpha\to\pi/2} \frac{d}{\cot(\alpha)} = \lim_{\alpha\to\pi/2} \frac{d'}{-(\csc(\alpha))^2} =$$

$$-d' = r \qquad (3\text{-}2)$$

In Eq. (3-2), $\cot(\cdot)$ is the cosine function, $\csc(\cdot)$ is cotangent function, and d' is the derivative of d with respect to α. From Eq. (3-2), we obtain the differential equation:

$$d' = -r \qquad (3\text{-}3)$$

Solve this differential equation:

$$d = k - r\alpha \qquad (3\text{-}4)$$

In Eq. (3-4), k is a constant. Since it is a constant, let:

$$k = k_1 r \qquad (3\text{-}5)$$

Substituting Eq. (3-5) into Eq. (3-4), we get:

$$d = r(k_1 - \alpha) \qquad (3\text{-}6)$$

Substituting Eq. (3-6) into Eq. (3-1), we get:

$$\lim_{\alpha\to\pi/2} \frac{r(k_1-\alpha)}{\cot(\alpha)} = r \qquad (3\text{-}7)$$

In Eq. (3-7), the denominator is 0, and the extreme value is a constant, so the numerator must also be 0, so: $k_1 = \pi/2$. That is:

$$\mathrm{d} = r(\pi/2 - \alpha) \qquad (3\text{-}8)$$

Substituting Eq. (3-8) into Eq. (3-1), we get:

$$x = r(\pi/2 - \alpha)\tan(\alpha)$$

End Proof.